Available online at www.sciencedirect.com
SCIENCE DIRECT®

Journal of the European Ceramic Society 24 (2004) 3139–3148

www.elsevier.com/locate/jeurceramsoc

The formation of refractory oxide coatings on Nicalon™ fiber by sol-gel process

N.I. Baklanova[a,*], T.M. Zima[a], T.M. Naimushina[a], S.V. Kosheev[b]

[a]*Institute of Solid State Chemistry and Mechanochemistry, SB RAS, Novosibirsk 630128, Russia*
[b]*Boreskov Institute of Catalysis, SB RAS, Novosibirsk 630090, Russia*

Received 16 July 2003; accepted 4 October 2003

Abstract

Sols of alumina, zirconia, titania and their mixes may be used as simple and readily processable precursors for ceramic interfacial coatings on SiC-based Nicalon™ fibers. The morphology, composition and tensile properties of coated fibers were evaluated for different systems in dependence of processing conditions by SEM, XPS, XRD analysis. All coatings obtained are uniform, continuous and adherent to substrates. They are distinguished by their morphological features, tensile strength, thermal resistance and compatibility with fiber. The peculiarities of the behavior of oxide-coated fibers are governed by the properties of initial sols, procedure for coating fabrication, chemical and nanostructural factors.

Keywords: Coatings; Fibres; Interfaces; Nicalon fibre; Oxide coatings; Sol-gel processes

1. Introduction

Silicon carbide-based ceramic matrix composites (CMCs) are leading candidate materials for high-temperature structural applications such as heat exchangers and advanced gas turbine engines.[1] It is well established that the mechanical properties of CMCs strongly depend on the fiber–matrix bonding. The improvement of the mechanical properties of CMC's is achieved through the interposition of interphase materials such as carbon and *hex*-BN. The carbon and *hex*-BN interfacial coatings on the fibers exhibit some instability in oxidizing environment.[2–4] There is a strong interest to study the feasibility of utilizing oxide interphase materials that are chemically stable towards an oxidizing environment.

A modern concept of interphase design is based on multilayered system consisting of several layers, one of which is a refractory oxide. Refractory oxide fiber coatings are most commonly used on oxide fibers. The application of oxide fiber coatings on silicon carbide based fibers has generally been avoided because these fibers can react with oxide coatings. However, there are several examples of refractory oxides used as promising candidates coating materials.[5–8] Callender et al.[5] have produced metal-doped alumina coatings on SiC and carbon fibers. The coatings derived from alumoxane precursors were uniform and stable to thermal cycling under air at 1000–1400 °C and during repeated thermal cycling. The oxidation of the SiC fiber substrate was not detected. A group of interfacial materials including calcium-, lanthanum-doped aluminates has been proposed by Cinibulk.[6] The interlayers were not only oxidation resistant, but chemically compatible with composite constituents. ZrO_2 coating on ceramic fiber substrates such as Hi-Nicalon™ was deposited and characterized by Borst et al.[7] They showed that the ZrO_2-coated fiber clothes remained flexible, suggesting that the fibers did not become significantly embrittle during the coating process. Lara-Curzio et al.[8] reported an effective interphase system for SiC fiber consisting of $SiO_2/ZrO_2/SiO_2$ layers. After a 10 h oxidation treatment at 960 °C the $SiO_2/ZrO_2/SiO_2$ interphase exhibited excellent chemical stability as evidenced by the preservation of their sharp interphase boundaries. No diffusion of silicon and zirconium within multilayered

* Corresponding author. Tel.: +7-3832-363839; fax: +7-3832-322847.
E-mail address: baklanova@solid.nsc.ru (N.I. Baklanova).

0955-2219/$ - see front matter © 2003 Elsevier Ltd. All rights reserved.
doi:10.1016/j.jeurceramsoc.2003.10.004

structure, as well as no carbon as an impurity phase in interphase region was observed.

The aim of the present work is (1) to study the particularities of the formation of refractory oxide interfacial coatings on Nicalon™ fibers by sol-gel technique and (2) to characterize the barrier coatings on Nicalon™ fibers. ZrO_2, TiO_2, Al_2O_3, and their double oxides are the most promising candidates for interfacial coatings. Sol-gel process is one of the most convenient and low-cost techniques to produce oxide coatings.[9] This is because of the possibility of using liquid solutions to fabricate films with an extremely wide range of chemical composition, structure, texture and porosity in dependence on processing variables. Solution-based precursors allow accurate stoichiometric control and convert to desired phases at low temperatures upon decomposition.

2. Experimental procedure

2.1. Coating preparation

Precursors for oxide and complex oxide nanosized coatings were the sols of hydrated aluminium oxide (HAO), zirconium dioxide (HZDO), titanium dioxide (HTDO) and their binary mixtures. The sols were synthesized electrochemically from aqueous solutions of metal oxychlorides. Before coating procedure the sols were aged for 2–3 months. Binary sols were prepared by mixing the corresponding sols in 1:1 (mol.) ratio at intensive stirring and were used to coating process after a 5 min. The concentration of dispersive phase was varied by diluting. Rheological characterization of initial sols was performed on rotary viscometer "Reotest-2.1" at 25 °C, with a concentric cylinder geometry. Shear measurements were performed at 1–1000 s^{-1} by incrementing the shear rate and measuring the shear stress after a determined equilibration time at each shear rate. For rheological studies the sols were concentrated by water evaporation at 40 °C.

Nicalon™ NLM202 (Nippon Carbon) SiC based woven fabric was used as substrate for oxide interfacial coatings. Before deposition, the fibers were desized according to standard procedure. The fabric was immersed for 24 h in 50:50 acetone/ethanol mixture in order to remove the sizing agent, then fibers were thermally treated in air at 450 °C and vacuum at 960 °C for 1 h.

The coating process was based on the dipping of Nicalon™ fabrics into sols of hydrated oxide metals. To increase coating thickness, multiple depositions were used with drying at ambient temperature in air and then at 960 °C in vacuum or argon between depositions. The major drawback of solution-based coating process is a difficulty in obtaining bridge-free coatings. Special technique analogous to infiltration process allowed us to minimize the fiber bridging problem. The technique was applied to wetted fabrics to displace excess coating solution that is normally retained between monofilaments within a tow bundle after dipping in sols.

2.2. Coating characterization

X-ray diffraction (XRD) measurements were conducted using monochromatic Cu-K_α radiation with DRON-3 diffractometer (Russia). Scanning electron microscopic (SEM) analysis was carried out using a JSM T-20 (Jeol) and BF-350 (Tesla) with a resolution of 5 nm.

The electronic structure of coatings was characterized by XPS using a VG ESCALAB spectrometer equipped with facilities to obtain the surface depth profile. XPS spectra were recorded using Al-K_α irradiation and calibrated against $Au4f_{7/2}$ (BE = 84.0 eV) and $Cu2p_{3/2}$ (BE = 932.7 eV) lines. All spectra are presented in binding energy scale that was obtained with respect to C 1s peak of carbon at 285.0 eV. For spectroscopic analysis of electron spectra the original software CALC was applied to extract the detailed information about electron structure of materials.

2.3. Tensile strength measurements

Room-temperature tensile tests of the individual filaments were performed in ambient atmosphere using a fiber testing machine FM-27 (Hungary). Single fibres were glued with epoxy resin on a tab holder. The side portions of tab were cut with a hot wire just before application of the load. Measurements were carried out at a constant crosshead speed of 1.2 mm/min, the gauge length was 10 mm. A load cell with a sensitivity range of 50 cH was used to measure the failure load. Ten filaments of each type of fibers were tested. The average diameter of each type of fibers was measured prior to tensile testing by laser interferometry.

3. Results

3.1. Rheological properties of sols

One can see from Fig. 1a, b, c that the rheological properties of the initial sols are notably distinct from each other. The dependences of effective viscosities of HZDO on shear strain for different concentrations are represented in Fig. 1a. It appears that a small (up to ~20% mass loss of water) increase of the sol concentration leads to a substantial increase of viscosity, especially at deformation rate below 500 s^{-1}. The viscosity of the initial HAO sol is small and only slightly dependent on the deformation rate. Concentrating HAO sol by water evaporation has an effect on the character of

flow only when more than 70% (wt.) of water is lost. The sol loses fluidity at about 80% (wt.) loss of water. For aged HTDO sol, rather weak non-linear increase in the equilibrium transverse strain with an increase in deformation rate is observed within the whole investigated range (Fig. 1c). Newton character of flow in the aged HTDO sol is conserved after its concentrating (water loss of 70–80% wt.). Thus, a characteristic feature of the aged sol is insignificant degree of structuring.

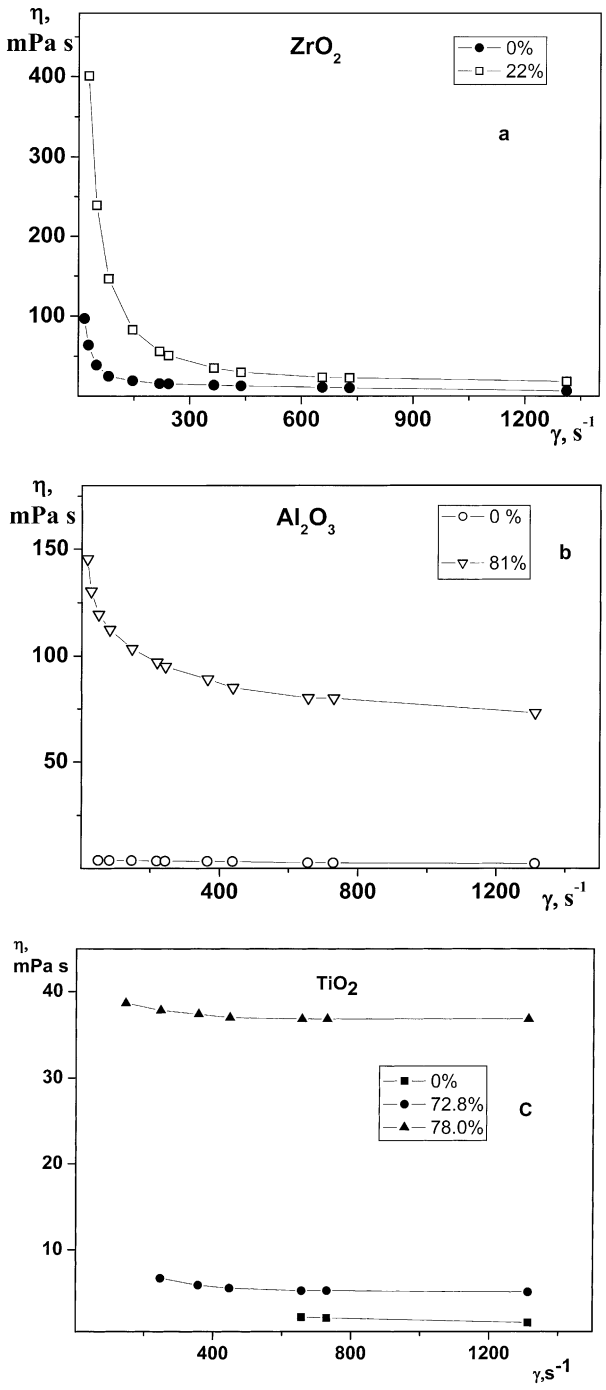

Fig. 1. The dependences of effective viscosities of sols on shear strain for different concentrations: a—ZrO_2; b—Al_2O_3; c—TiO_2.

An increase of the number of dipping-annealing cycles up to three leads to a monotonous increase of the fiber mass (Fig. 2). Further cycles give almost zero mass gain. Moreover, for Al_2O_3 and Al_2O_3/ZrO_2 coatings, the monotonous character of the dependencies is distorted, which could be connected with the peeling and crumbling of coatings.

3.2. SEM and XRD analysis

The SEM micrographs from the surface of the Al_2O_3-coated Nicalon™ fibers after one cycle dipping-annealing are shown in Fig. 3a, b, c. The coating derived from dilute alumina sol is very smooth, thin, rather uniform over diameter of monofilament. A higher magnification reveals that the alumina particles are platelets (Fig. 3b). They are more aligned parallel to the fiber surface. The other features of the alumina coating are texturization and porosity. The size of particles and pores, determined from the SEM micrographs with the Image-Pro Plus software, is about 30–50 nm. However, there are macro pores in the coating of some filaments. No fiber bridging, no spalling of coating was observed. The thickness of coating after the first cycle, determined by SEM, is 0.08–0.1 μm. An increase of the number of cycles leads not only to the increase of the thickness of coating till about 0.12 μm for three cycles but also to the change of the morphology. The appearance of non-uniformities shaped as crystallized traces of coating sol that was retained between fibers within a tow bundle is seen on the surface of some filaments (Fig. 3c). The alumina coating remains X-ray amorphous even after six dipping-annealing cycles.

The SEM micrographs of the surface and cross-section of ZrO_2-coated Nicalon™ fibers are shown in Fig. 4a, b. The coating on Nicalon™ fiber of the 0.08–0.1 μm thickness is composed of round particles about

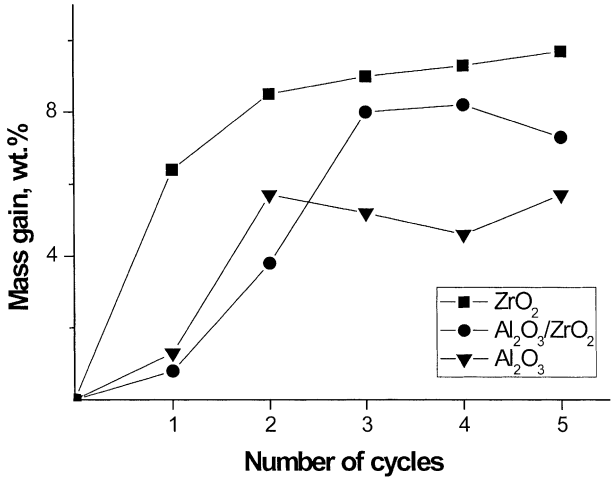

Fig. 2. Plot of mass gain of coated fiber versus the number of dipping-annealing cycles.

30–50 nm in size. Pore size determined from SEM images is also about 30–50 nm. It is a free-crack coating. One can see from Fig. 4b, that there is a sharp boundary between coating and fiber. No macro defects such as bubbles and fiber bridging were observed. According to XRD analysis, the appearance of a mixture of the monoclinic and tetragonal modifications can be detected after the third cycle (Fig. 5a).

The morphology of the Al_2O_3/ZrO_2 coating on Nicalon™ fiber is analogous to that of the ZrO_2 coating. It is dense and nanosized (Fig. 6). There are macro non-uniformities on the surface, shaped as craters with the walls built of well faceted crystals. After the sixth dipping-annealing cycle, only peaks belonging to the tetragonal ZrO_2 phase are observed in X-ray diffraction patterns (Fig. 5b).

The SEM images of the TiO_2 and Al_2O_3/TiO_2 coatings derived from corresponding dilute sols are shown in Fig. 7a and b, respectively. The appearance of a mixture of anatase and rutile phases in the coating derived from undiluted TiO_2 sols became detectable by XRD analysis only after several dipping-annealing cycles (Fig. 8a). The coating derived from dilute TiO_2 sol is the X-Ray amorphous one. The main feature of the Al_2O_3/TiO_2 coating is the presence of anatase only instead of mixture of anatase and rutile phases (Fig. 8b).

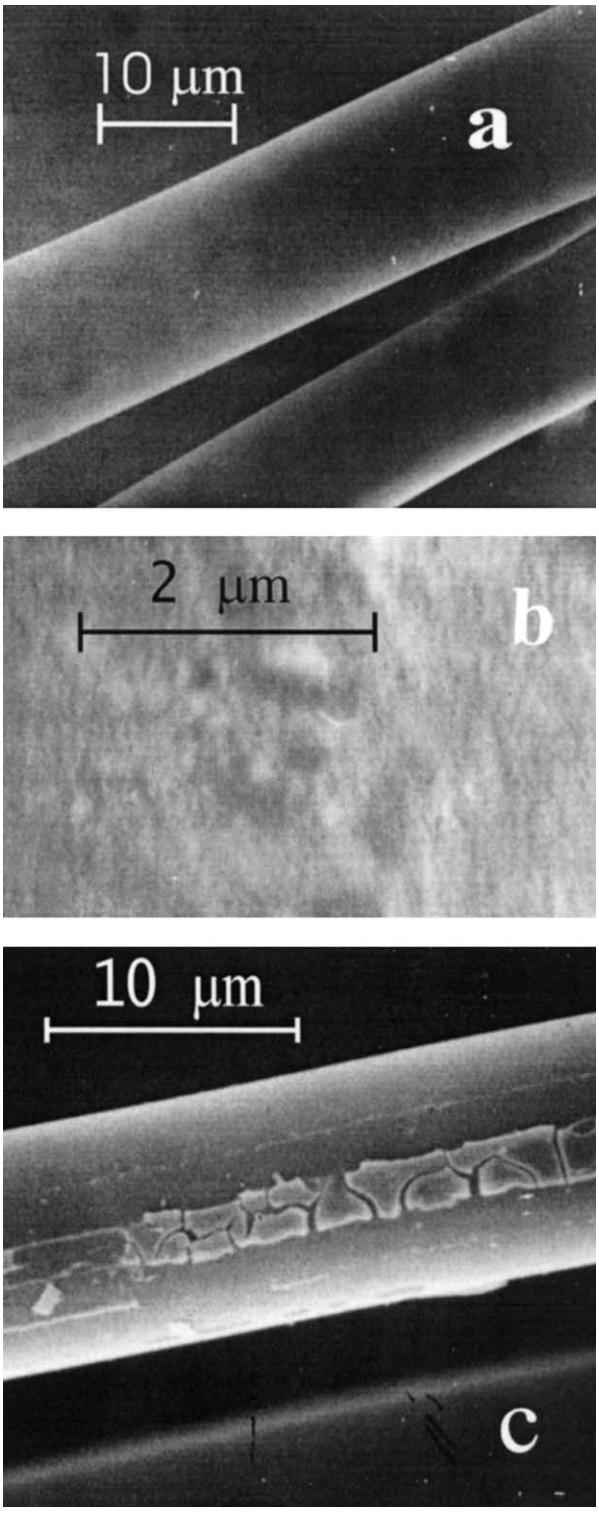

Fig. 3. SEM images of the Al_2O_3-coated Nicalon™ fibers.

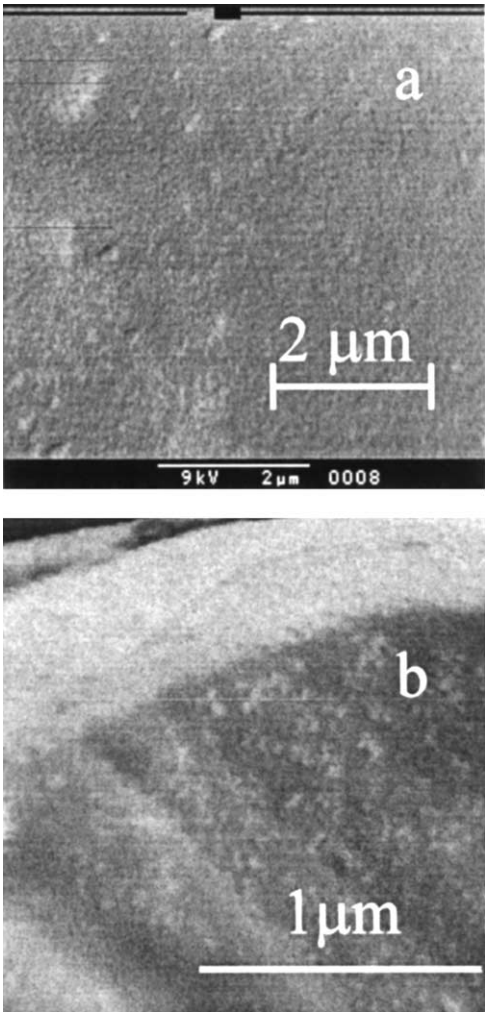

Fig. 4. SEM images of surface (a) and cross-section (b) of ZrO_2-coated Nicalon™.

The composition of coatings obtained by dipping of Nicalon™ in mixture of TiO_2 and ZrO_2 sols is represented by $ZrTiO_4$, the appearance of this phase being detectable after several dipping-annealing cycles by X-ray diffraction.

The treatment of oxide coated Nicalon fabrics under high-vacuum and high-temperature (1200 and 1350 °C) for 2 h results in a coarse-grained radial textured structure of coated fibers (Fig. 9a). The surface morphology of Al_2O_3/TiO_2 coated Nicalon™ fiber is changed slightly at high-temperature treatment (Fig. 9b).

3.3. XPS analysis

XPS survey spectra recorded from desized and coated Nicalon™ fabrics revealed carbon, silicon, oxygen, zirconium, aluminum as main components. After correcting the intensities of C1s, O1s, Si2p, Al2p and $Zr3d_{5/2}$ photopeaks for their atomic sensitivity factors (ASF) the composition of surface of fabrics could be evaluated. The elemental compositions and binding energies (BE) for the Al_2O_3-, ZrO_2-, Al_2O_3/ZrO_2-coated Nicalon™ fabrics are presented in Table 1. It should be noted that the reported compositions should be considered as indicative of mean values because of differences between various batches of Nicalon™ fibres. One can see from Table 1 that the common feature of coatings is the presence of silicon dioxide as main component. The compositions of the Al_2O_3/ZrO_2 coatings obtained by different ways only slightly differ from each other. Asymmetry of the C1s, Si2p, and O1s peaks show that these signals do not correspond to unique chemical

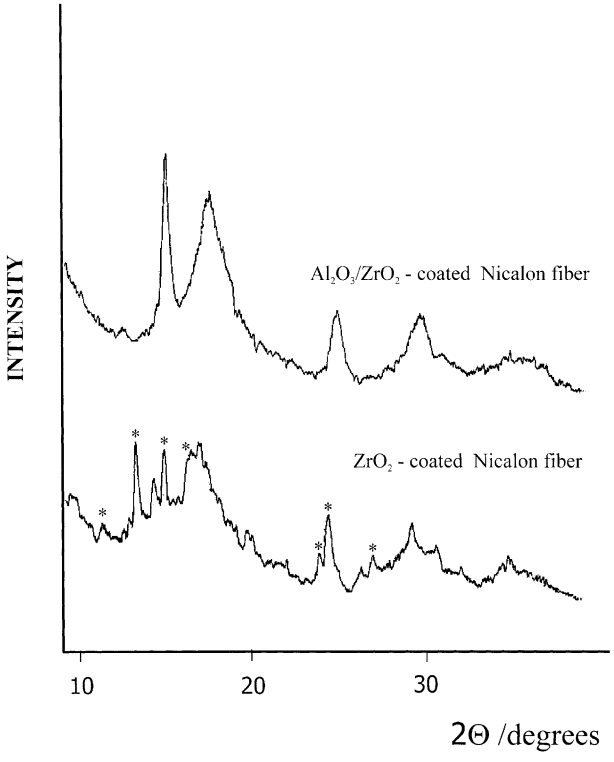

Fig. 5. XRD data of coated Nicalon™ fibers: a—ZrO_2; b—Al_2O_3/ZrO_2.

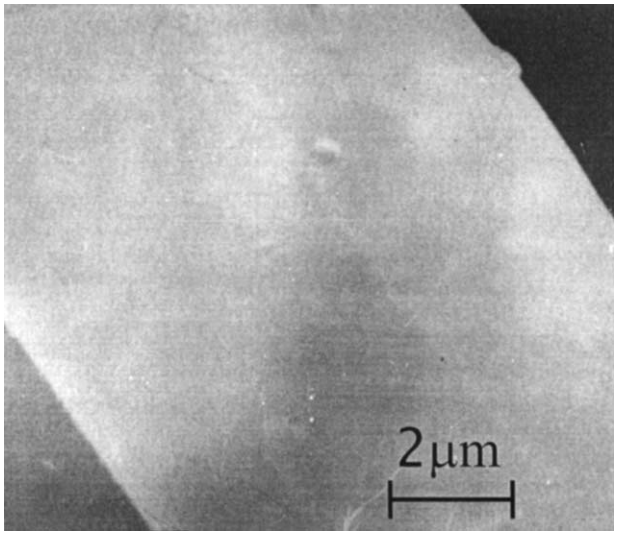

Fig. 6. The Al_2O_3/ZrO_2 coating on Nicalon™ fiber.

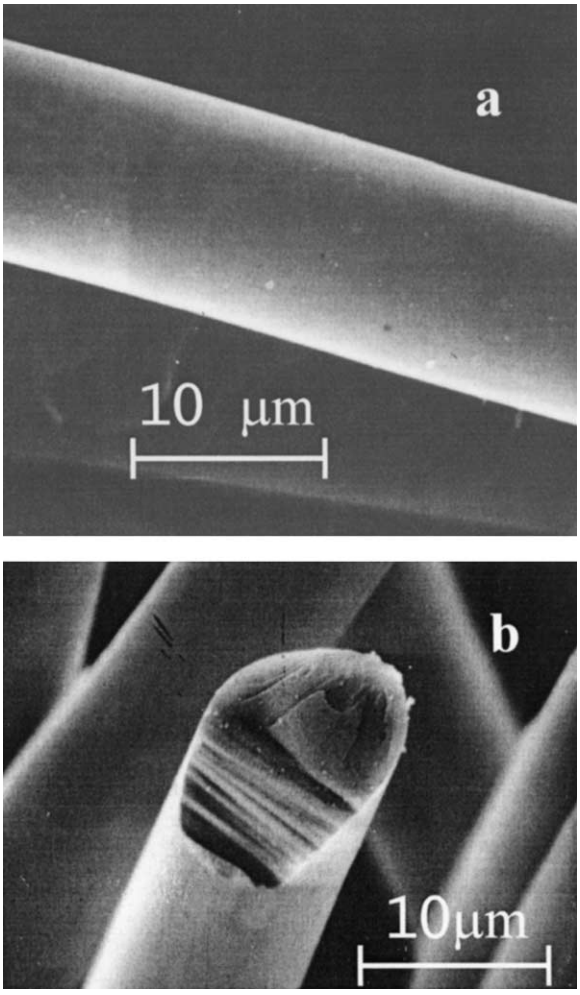

Fig. 7. SEM images of coated fibers: a—TiO_2; b—Al_2O_3/TiO_2.

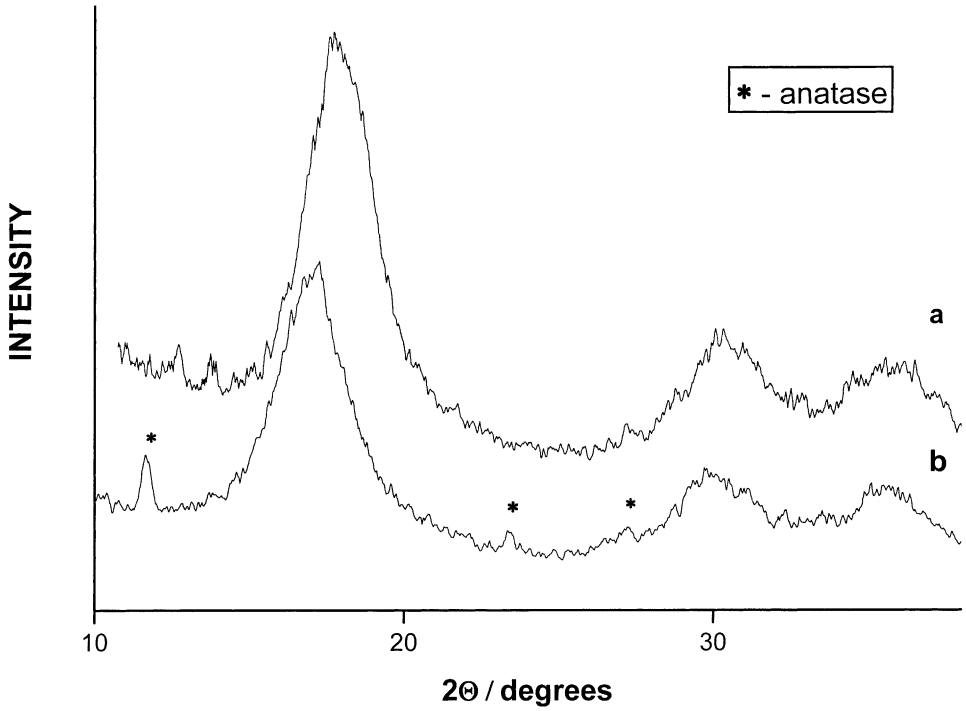

Fig. 8. XRD data of coated Nicalon^{TM} fibers: a—TiO_2; b—Al_2O_3/TiO_2.

state and several phases present in the surface layer. Asymmetry and slight shift of the O1s photopeak for oxide-coated Nicalon^{TM} fabrics in comparison with uncoated Nicalon^{TM} are an evidence of the presence of several oxide phases in coatings (Fig. 10a). The feature became noticeable especially for ZrO_2-coated Nicalon^{TM}. The appearance of the O1s photopeak (530.5 eV) as shoulder in the spectrum of ZrO_2-coated Nicalon^{TM} indicates the presence of ZrO_2 together with SiO_2 (Fig. 10b). The location of the O1s peak is in a good accordance with the value reported by Moulder et al.[10] for ZrO_2. Asymmetry of the peak at 530.5 eV is absent and it is an evidence of unique zirconium oxide form.

3.4. Tensile strength of coated Nicalon^{TM} fibers

Results of tensile strength testing of coated and uncoated Nicalon^{TM} fibers are represented in Fig. 11. The procedure of removing the sizing agent appear to cause a decrease in the strength of Nicalon^{TM} fiber. Moreover, the failure strength of desized and thermal treated in argon Nicalon^{TM} fiber is lower than that of only desized fiber. The coating procedure results in the succeeding decrease in strength of single-filaments. One can see, that increasing the number of dipping-annealing cycles is followed by an appreciable decrease in tensile strength of coated single-filament for each type of coating. Strength of monofilaments with coatings is also dependent on the concentration of sol which is used to deposit the coating. Monofilaments with the coatings obtained from diluted Al_2O_3 sols exhibit strength that differs only slightly from that for the initial fiber but exceeds that for the coated fibers obtained from non-diluted sols. A similar dependence of strength on the concentration of the sol is observed also for Al_2O_3/TiO_2 coatings on Nicalon^{TM} (Fig. 11).

4. Discussion

As we can see above, using the sols of hydrated oxides of aluminum, zirconium, titanium and their mixtures makes it possible to produce very thin, uniform, nanostructured ceramic coatings on Nicalon^{TM} fibers. This coating technique relies on wetting of fiber cloth by sols. It is known that on the Nicalon fiber surface the layer of SiO_2 is present.[11] A key characteristics of the SiO_2 surface is that the so-called residual valences react with water, so that at room temperature the surface becomes coated with silanol (SiOH) groups.[12] The wetting of the fiber surface is provided by the physical adsorption due to Van-der-Vaals forces and chemisorption due to interaction of chemically active functionalities on the surface of Nicalon^{TM} fiber such as SiOH groups and the hydrated particles of sols. The electrostatic attraction between the positively charged MeO_n particles and the negatively charged fiber cloth surface is also to be taken into attention. The adherence of sol-gel derived oxide coatings to fiber is affected by all of the processing stages: coating solution preparation, deposition and drying, thermal treatment.[9] Among many factors affecting microstructure of a coating, chemical and

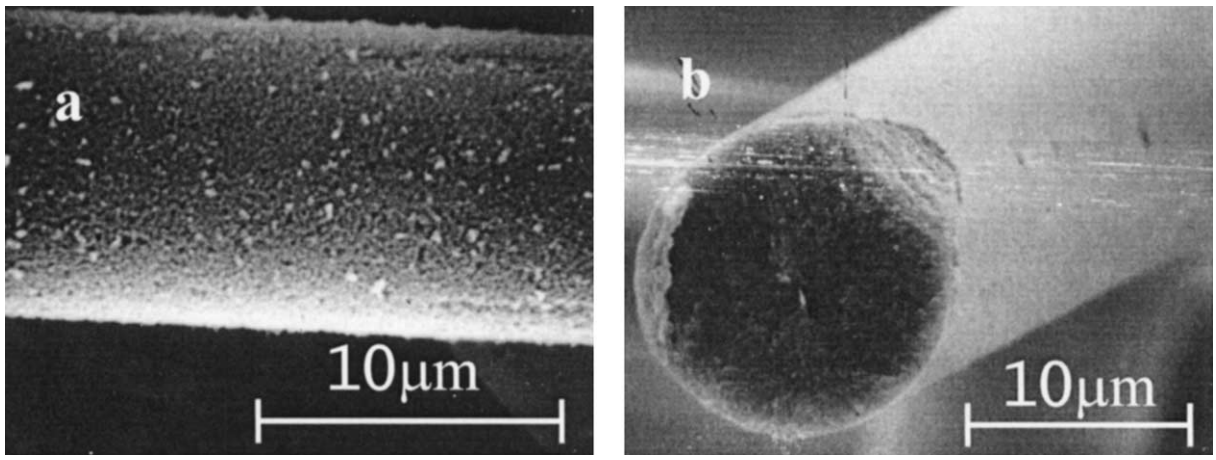

Fig. 9. SEM images of coated fibers treated at 1350 °C: a—the Al_2O_3/ZrO_2 and b—Al_2O_3/TiO_2.

Table 1
Elemental atomic compositions and binding energies for coated Nicalon™ fibers

Specimen	Composition (at.%) binding energy (eV) between ( )				
	Si	C	O	Al	Zr
Initial Nicalon	23.20	13.37	63.44		
	(103.6	285.0	533.0)		
Al_2O_3-coated Nicalon	21.20	19.71	57.80	1.30	
	(103.1	285.0	532.3	75.1)	
ZrO_2-coated Nicalon	14.96	26.87	52.90		5.26
	(103.4	285.0	530.5		182.6)
			532.6		
Al_2O_3/ZrO_2-coated Nicalon[a]	18.72	19.10	60.21	0.19	1.79
	(103.1	285.0	532.4	74.9	182.6)
Al_2O_3/ZrO_2-coated Nicalon[a]	18.72	20.45	58.56	0.28	1.99
	(103.2	285.0	532.4	75.0	182.8)

[a] Obtained by different ways.

rheological properties of the initial sols are most essential.

Previously, it was shown by Zima et al.[13] that the primary particles in the ash of hydrated zirconium dioxide were spherical with the diameter of 2–3 nm. While concentrating, the viscosity of zirconium oxide sol increases sharply even at not very high concentrating extent. This is accompanied by polycondensation reaction with the removal of water. Due to the continued condensation reactions, the semi-rigid network becomes more cross-linked. Such a condensation process is characteristic of hydroxo-aquo precursors ($[Me(OH)_x(OH_2)_{N-x}]^{(z-x)+}$).[14] Hydroxo-bridges are formed through oxygen atoms from hydroxyl groups. At lower temperatures condensation among hydroxyls located primarily within the skeleton is the predominant mechanism. In contrast, surface hydroxyls are involved at higher temperatures. As the curing temperature increases, the double hydroxyl bonds in the polymeric structure are converted to oxo bonds [i.e., Zr–O–Zr]. Such a behavior of the system leads to insignificant shrinkage of the coating and the formation of porous and thick coatings composed of zirconium oxide. The thickness of the resulting coating is about 0.1 μm, as was determined with help of SEM analysis.

As was mentioned above, multiplying the number of repeated dipping-thermal treatment cycle leads to the formation of a ZrO_2-based coating on Nicalon™, consisting of a mixture of the monoclinic and tetragonal phases (Fig. 5a). The observation of metastable tetragonal ZrO_2 phase below the monoclinic-tetragonal transition temperature (approximately 1200 °C) was reported in several works.[15–17] It was shown that the stability of tetragonal ZrO_2 results from lattice defects, specifically oxygen vacancies, created upon crystallization from alkoxide and zirconyl chloride solutions. A sufficient decrease in the number of these vacancies due to heat treatment in the presence of oxygen facilitates the instability in the metastable tetragonal phase and the following $t \rightarrow m$ transition.[15] An analogous phenomenon was observed not only for monolithic ceramic specimens but also within the CVD ZrO_2

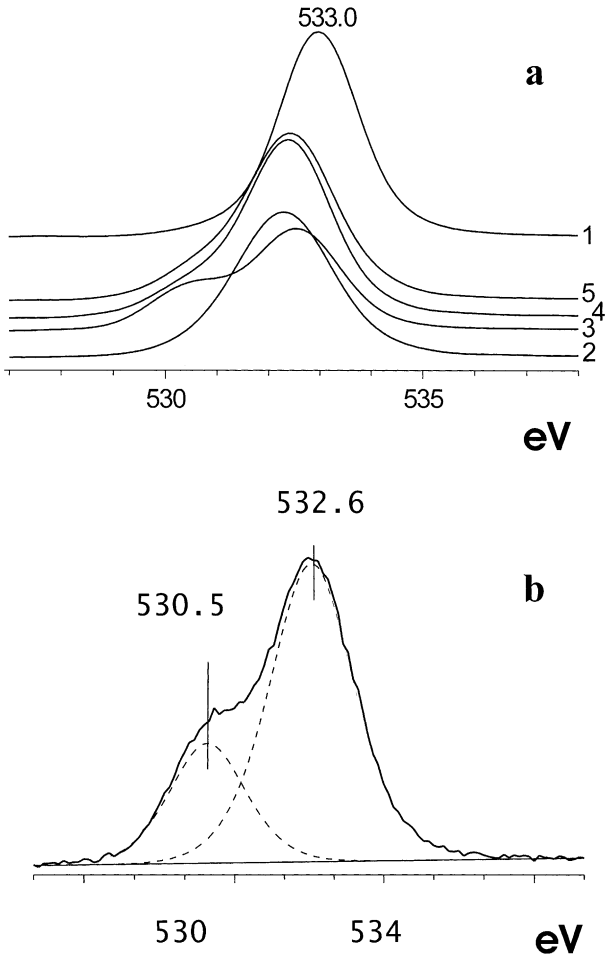

Fig. 10. XPS for Nicalon™ fiber: a—O1s photopeaks of the initial Nicalon™ (1); Al_2O_3-coated (2); ZrO_2-coated (3); Al_2O_3/ZrO_2 -coated by different ways (4,5); b—O1s deconvoluted photopeak for ZrO_2-coated Nicalon™.

coating on SiC fiber by Li et al.[18] Besides above-mentioned factors the influence of support, namely, SiC fiber and also free carbon presenting as an impurity in coating on the mechanism of tetragonal ZrO_2 phase nucleation must be taken into consideration.

Quite different behavior is observed during the formation of alumina coating. One can see in Fig. 2 that the viscosity of the sol changes only slightly till high concentrating extent. This may be due to the formation of the more-open, less-cross-linked network. Such behavior leads to the formation of flat crystalline Al_2O_3 particles directed parallel to the fiber surface. The coating conserves its X-ray amorphous character even after six impregnation-annealing cycles, so it is difficult to identify the formed modifications of aluminium oxides. These morphological peculiarities appear to be the reason for enhanced strength of Al_2O_3 coated Nicalon™ fiber in comparison with as-received one. Earlier analogous interfacial behaviour was observed for ZrO_2 coating on SiC fiber by Li et al..[18] They noted that the fiber tow failure load was not degraded because (1) the overall thickness was below 100 nm, and (2) the fiber surface was not covered continuously by ZrO_2.

According to XPS data, the composition of Al_2O_3/ZrO_2 coating is represented by a mixture of zirconia and alumina. In accordance with XRD analysis, the coating obtained after five impregnation-annealing cycles contains only tetragonal modification of ZrO_2, no peaks belonging to monoclinic phase was observed. The stability of tetragonal ZrO_2 particles in ceramic matrixes was considered thoroughly by Heuer et al.[19,20] They showed that the stability of tetragonal ZrO_2 in Al_2O_3–ZrO_2 composites is due to a "critical" size of ZrO_2 particles that can be transformed into monoclinic phase and larger particles undergo the martensitic $t \rightarrow m$ transformation more readily than do smaller particles. The presence of Al_2O_3 phase in coating can inhibit the grain growth of ZrO_2 particles, thus resulting into stabilization of tetragonal phase. The chemical effects, namely, a larger solubility for Al_2O_3 in t-ZrO_2 than in m-ZrO_2 cannot be disregarded at this time.

As mentioned above, we observed the appearance of macro non-uniformities in the coating, shaped as well faceted crystals (Fig. 6). According to phase equilibria of the Al_2O_3–ZrO_2–SiO_2 system,[21] no ternary compounds and solid solutions of any detectable concentrations are formed. The appearance of macro non-uniformities can be connected with the formation of mullite as result of interaction of Al_2O_3 and SiO_2 that is present on the Nicalon™ surface (Table 1). According to,[21] mullite is crystallized often as needles. The formation of zircon phase in the temperature range up to 1000 °C is unlikely. As was mentioned above, due to close values of BE O1s for SiO_2 and Al_2O_3 it is difficult to draw a conclusion from the XPS results about nature of interfacial layer.

The peculiarity of the ZrO_2–TiO_2 coatings on Nicalon™ fiber is the presence of the $ZrTiO_4$ phase. Early, Newport et al.[22] thoroughly studied the ternary ZrO_2–TiO_2–SiO_2 xerogels having various Zr:Ti:Si ratios and found that only system with a minority of Zr shows the presence of phase separation attributed to the formation of $ZrTiO_4$. In systems with higher zirconium content the crystallization of ZrO_2 phase was observed. In our work the sol-gel processing conditions appear to provide direct crystallization into $ZrTiO_4$ at temperature lower than 1000 °C. Despite the fact that the Zr:Ti ratio in the mixture of the initial sols was about 1:1 the real Zr:Ti ratio in coating might be different due to (i) different rheological properties of the zirconia and titania sols and (ii) different character of interaction of the initial sols with Nicalon™ fiber as support.

Further investigations of the ZrO_2–TiO_2 coatings on Nicalon™ fiber are necessary to evaluate the role of the $ZrTiO_4$ phase for thermal stability of the coated fibers. It is known that the phase transition in $ZrTiO_4$ can occur at about 1125 °C with a small (≈0.3%) increase in

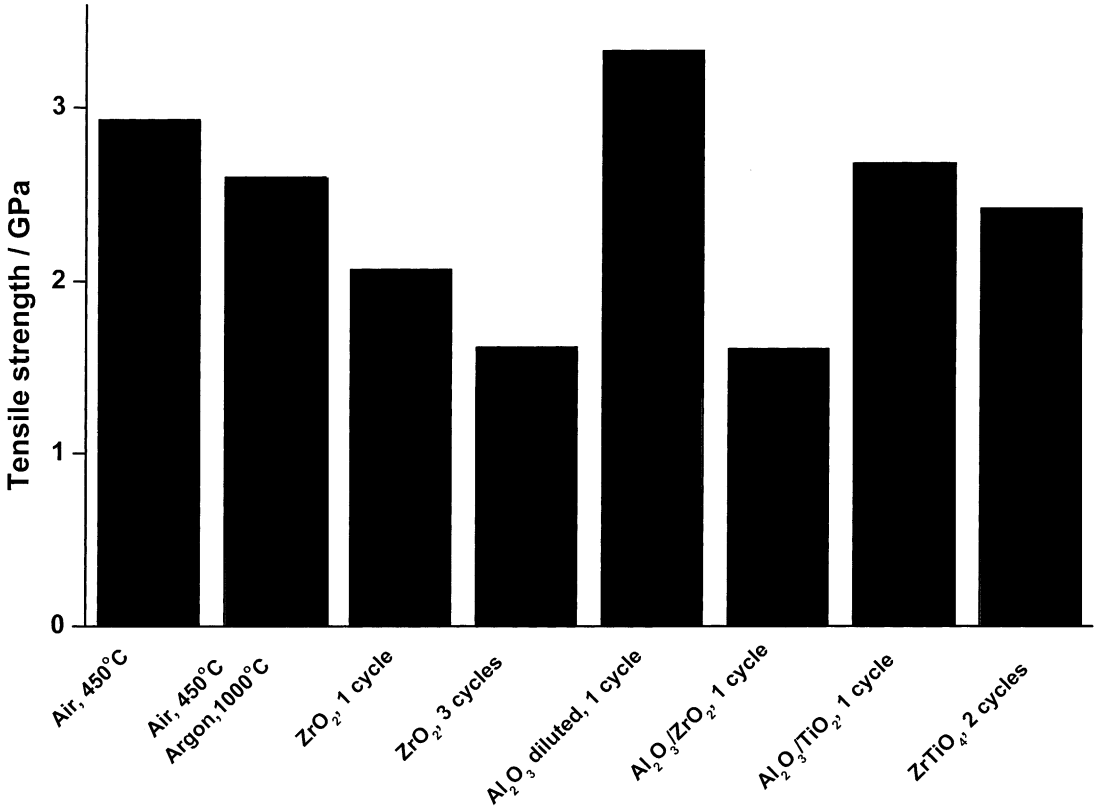

Fig. 11. Coated Nicalon™ monofilament tensile strengths measured at room temperature.

volume.[23] The other undesirable feature of this coating is the appearance of crystals, the sizes and number of which are increased with raising temperature. Crystals constitute rigid inclusions acting as defects and break the homogeneity within coating. This appear to result in low values of tensile strengths of the ZrO_2–TiO_2 coated fibers.

Unlike the mentioned above system, the sol-gel preparation of coating from mixture of HAO and HZDO sols resulted into a separate crystallization of Al_2O_3 and TiO_2 phases. The formation of Al_2TiO_5 at temperatures as low as 1000 °C was not detected. Early it was noted by Andrianainarivelo et al.[24] that aluminium titanate can be obtained at low temperatures when homogeneous gels has been formed. An absence of direct crystallization of Al_2TiO_5 and the intermediate formation of alumina and titania appear to be due to a non-homogeneous sol that is formed after mixing of the initial HAO and HZDO sols. Heating of coated fibers up to 1300 °C for obtaining of Al_2TiO_5 by solid state reaction between Al_2O_3 and TiO_2 phases within coating did not yield positive results. According to Freudenberg et al.[25] this solid state reaction becomes noticeable only at temperatures higher than 1300 °C. Karakhchiev et al.[26] also observed the crystallization of separate oxide phases instead of Al_2TiO_5 during thermal treatment of binary alumina-titania sol that was obtained by direct electrochemical synthesis. It must be concluded that additional studies are required to obtain homogeneous binary hydrated alumina–titania sol.

The peculiarity of the Al_2O_3–TiO_2 coatings is the presence of only one phase, namely, anatase instead of mixture of the anatase and rutile phases that were observed in the TiO_2 based coating on Nicalon™ fiber. The stabilization of low temperature TiO_2 phase seems to be connected with the presence of alumina which can inhibit the growth of the TiO_2 particles to critical size as it was observed above for the Al_2O_3–ZrO_2 system. Inclusions can also inhibit the anatase- rutile transformation.[21] Lower tensile strengths of monofilaments with the Al_2O_3–TiO_2 coatings derived from undiluted sols in comparison with those derived from diluted ones can be connected to more rough microstructure, namely, rather large crystals within coating (Fig. 7b).

5. Conclusion

Sols of alumina, zirconia, titania and their mixes may be used as simple and readily processable precursors for ceramic interfacial coatings on SiC-based Nicalon™ fibers. The peculiarities of morphology, composition and tensile properties of coated fibers were evaluated for different systems in dependence of processing conditions. All coatings obtained are uniform, continuous and adherent to substrates. They are distinguished by

their morphology, tensile strength, thermal resistance and compatibility with fiber. The peculiarities of the behavior of oxide-coated fibers are governed by the properties of initial sols, procedure for coating fabrication, chemical and nanostructural factors. The important factor determining the behavior of the systems oxide coating—Nicalon™ fiber is silicon dioxide which is present on the surface of initial Nicalon™ fiber.

The obtained results allow us to consider the oxide-based coatings as candidates for interphases for applications in ceramic matrix composites.

Acknowledgements

The authors are grateful to Mrs. T.A. Gavrilova and Dr. M.A. Korchagin for SEM analysis.

References

1. Lee, K. N. and Miller, R. A., Oxidation behavior of mullite-coated SiC and SiC/SiC composites under thermal cycling between room temperature and 1200–1400 °C. *J. Am. Ceram. Soc*., 1996, **79**(3), 620–626.
2. Fillipuzzi, L., Camus, G., Naslain, R. and Thebault, J., Oxidation mechanisms and kinetics of 1D-SiC/C/SiC composite materials: I, experimental approach. *J. Am. Ceram. Soc*., 1994, **77**(2), 459–466.
3. Naslain, R., Dugne, O., Guette, A., Sevely, J., Brosse, Ch.R., Rocher, J.-Ph. and Cotteret, J., Boron nitride interphase in ceramic-matrix composites. *J. Am. Ceram. Soc*., 1991, **74**(10), 2482–2488.
4. Sheldon, B. W., Sun, E. Y., Nutt, S. R. and Brennan, J. J., Oxidation of BN-coated SiC fibers in ceramic matrix composites. *J. Am. Ceram. Soc*., 1996, **79**(2), 539–543.
5. Callender, R. L. and Barron, A. R., Novel route to alumina and aluminate interlayer coatings for SiC, carbon and Kevlar® fiber-reinforced ceramic matrix composites using carboxylate-alumoxane nanoparticles. *J. Mater. Res*., 2000, **15**(10), 2228–2237.
6. Cinibulk, M. K., Microstructure and mechanical behavior of an hibonite interphase in alumina-based composites. *Ceram. Eng. Sci. Proc*., 1995, **16**(5), 633.
7. Borst, M. A., Lee, W. Y., Zhang, Y. and Liaw, P. K., Preparation and characterization of chemically vapor deposited ZrO_2 coating on nickel and ceramic fiber substrates. *J. Am. Ceram. Soc*., 1997, **80**(6), 1591–1594.
8. Lee, W. Y., Lara-Curzio, E. and More, K. L., Multilayered oxide interphase concept for ceramic-matrix composites. *J. Am. Ceram. Soc*., 1998, **81**(3), 717–720.
9. Francis, L. F., Sol-gel methods for oxide coatings. *Mater. Manufac. Proces*., 1997, **12**(6), 963–1015.
10. Moulder, J. F., Stickle, W. F. and Sobol, P. E., *Handbook of X-Ray Photoelectron Spectroscopy*. Perkin-Elmer Co., Physical Electronics Division, Eden Prairie Minnesota, 1992.
11. Porte, L. and Sartre, A., Evidence for a silicon oxycarbide phase in the nicalon silicon carbide fibre. *J. Mater. Sci*., 1987, **24**, 271–275.
12. Iler, R. K., *Chemistry of Silica. V.2*. John Wiley and Sons, New York, 1979.
13. Zima, T. M., Karakchiev, L. G., Gaponov, Yu.A., Zaitsev, B. N. and Lyakhov, N. Z., Sol of the hydrated ZrO_2–TiO_2 system. *J. Colloids*, 2001, **63**(4), 470–475 (in Russian).
14. Geiculescu, A. C. and Rack, H. J., X-ray scattering studies of polymeric zirconium species in aqueous xerogels. *J. Non-Cryst. Solids*, 2002, **306**(1), 30–41.
15. Collins, D. E., Rogers, K. A. and Bowman, K. J., Crystallization of metastable tetragonal zirconia from the decomposition of a zirconium alkoxide derivative. *J. Eur. Ceram. Soc*., 1995, **15**(11), 1119–1124.
16. Tomaszewski, H. and Godwod, K., Influence of oxygen partial pressure on the metastability of undoped zirconia dispersed in alumina matrix. *J. Eur. Ceram. Soc*., 1995, **15**(1), 17–23.
17. Stachs, O., Gerber, Th. and Petkov, V., The formation of zirconium oxide gels in alcoholic solution. *J. Sol-Gel Sci. Techn*., 1999, **15**(1), 23–30.
18. Li, H., Lee, J. and Lee, W. Y., Effects of air leaks on the phase content, microstructure, and interfacial behavior of CVD zirconia on SiC fiber. *Ceram. Eng. Sci. Proc., B*, 2002, **23**(4), 261–268.
19. Heuer, A. H., Claussen, N., Kriven, W. M. and Ruhle, M., Stability of tetragonal ZrO_2 particles in ceramic matrices. *J. Am. Ceram. Soc*., 1982, **65**(12), 642–650.
20. Butler, E. P. and Heuer, A. H., X-ray microanalysis of ZrO_2 particles in ZrO_2-toughened Al_2O_3. *J. Am. Ceram. Soc*., 1982, **65**(12), C–206.
21. Berezhnoi, A. S., *Multicomponent Oxide Systems*. Naukova Dumka, Kiev, 1970.
22. Mounjoy, G., Holland, M. A., Gunawidjaja, P., Pickup, D. M., Wallidge, G. W., Smith, M. E. and Newport, R. J., Transition metal atom sites in ternary ZrO_2–TiO_2–SiO_2 xerogels. *J. Sol-Gel Sci. Techn*., 2003, **26**(1), 137–141.
23. McHale, A. E. and Roth, R. S., Investigation of the phase transition in $ZrTiO_4$ and $ZrTiO_4$–SnO_2 solid solutions. *J. Am. Ceram. Soc*., 1983, **66**(2), C18–20.
24. Andrianainarivelo, M., Corriu, R. J. P., Leclercq, D., Mutin, P. H. and Vioux, A., Nonhydrolytic sol-gel process: aluminium and zirconium titanate gels. *J. Sol-Gel Sci. Tech*., 1997, **8**(1/2/3), 89–93.
25. Freudenberg, B. and Mocellin, A., Aluminium titanate formation by solid state reaction of fine Al_2O_3 and TiO_2 powders. *J. Am. Ceram. Soc*., 1987, **70**(1), 33–38.
26. Karakhchiev, L. G., Avvakumov, E. G., Vinokurova, O. B., Gusev, A. A., Zima, T. M. and Lyakhov, N. Z., Comparison of sol-gel and mechanochemical techniques to preparation of disperse Al_2TiO_5. *Chemistry for Sustaining Development*, 2001, **9**(1), 27–34 (in Russian).